Journal of Pharmacokinetics and Pharmacodynamics, Vol. 34, No. 3, June 2007 (© 2007)
DOI: 10.1007/s10928-007-9053-5

Development of a Physiology-Based Whole-Body Population Model for Assessing the Influence of Individual Variability on the Pharmacokinetics of Drugs

Stefan Willmann,[1,3] Karsten Höhn,[2] Andrea Edginton,[1] Michael Sevestre,[2] Juri Solodenko,[2] Wolfgang Weiss,[2] Jörg Lippert,[1] and Walter Schmitt[1]

Received February 09, 2006—Final February 09, 2007—Published Online March 13, 2007

In clinical development stages, an a priori assessment of the sensitivity of the pharmacokinetic behavior with respect to physiological and anthropometric properties of human (sub-) populations is desirable. A physiology-based pharmacokinetic (PBPK) population model was developed that makes use of known distributions of physiological and anthropometric properties obtained from the literature for realistic populations. As input parameters, the simulation model requires race, gender, age, and two parameters out of body weight, height and body mass index. From this data, the parameters relevant for PBPK modeling such as organ volumes and blood flows are determined for each virtual individual. The resulting parameters were compared to those derived using a previously published model (P^3M). Mean organ weights and blood flows were highly correlated between the two models, despite the different methods used to generate these parameters. The inter-individual variability differed greatly especially for organs with a log-normal weight distribution (such as fat and spleen). Two exemplary population pharmacokinetic simulations using ciprofloxacin and paclitaxel as model drugs showed good correlation to observed variability. A sensitivity analysis demonstrated that the physiological differences in the virtual individuals and intrinsic clearance variability were equally influential to the pharmacokinetic variability but were not additive. In conclusion, the new population model is well suited to assess the influence of individual physiological variability on the pharmacokinetics of drugs. It is expected that this new tool can be beneficially applied in the planning of clinical studies.

KEY WORDS: population modeling; PBPK; simulation; pharmacokinetics; interindividual variability; generic model.

[1]Bayer Technology Services GmbH, Process Technology/Systems Biology, Building E41, D-51368 Leverkusen, Germany.
[2]Bayer Technology Services GmbH, Process Technology/Computational Solutions, D-51368 Leverkusen, Germany.
[3]To whom correspondence should be addressed. e-mail: Stefan.Willmann@Bayertechnology.com

INTRODUCTION

The pharmacokinetic behavior of a drug is affected by physiological properties of the individual receiving the drug. For example, gender, age, (excess) body weight, body mass index, tissue composition, or the function of the liver or kidney potentially impact the absorption, distribution, or elimination of a chemical compound and, thus, its pharmacodynamic effect. The gold standard for determining relevant covariates is the performance of a population pharmacokinetic study (1). These studies employ several tens to hundreds of subjects and produce large pharmacokinetic data sets. Using sophisticated statistical methods, correlations between pharmacokinetic model parameters and individual characteristics are sought. Major drawbacks of this approach are the considerable experimental effort involved and further, the predictability is limited to the range of parameters that were covered by the ensemble of subjects included in the study from which the population-PK correlations were determined. Thus, either the subjects must be carefully chosen to encompass a large range of relevant parameters, ones not necessarily known in advance, or the number of individuals must be very large to increase the probability that all important cases are covered. Alternative or accompanying approaches that allow for both an early assessment of the influence of physiological variability on the pharmacokinetic outcome or can be used for hypothesis generation and testing are therefore highly desirable.

Physiology-based pharmacokinetic (PBPK) modeling simulates pharmacokinetic profiles on the basis of compound structure related information and a number of relevant physiological input parameters of the individual, such as organ volumes, tissue composition, blood flow rates, and clearance (2–4). This technology has demonstrated its potential in the framework of toxicological risk assessment (5) as well as in the drug research and development process (6). Whole-body PBPK-models as for example the PK-Sim® model (2,7,8) (Bayer Technology Services GmbH, Germany) explicitly contain the physiological properties that influence the pharmacokinetics of a drug. Such a model is ideally suited to simulate pharmacokinetic variability by employing a range of gross physiological input parameters (e.g., weight, height, age). A prerequisite is that the variability of relevant properties within a population (e.g organ weights, blood flows) is known. If this is the case, a PBPK-model can be used to make *predictions* of pharmacokinetic behavior in specific virtual individuals or populations using realistic physiological properties. The use of predictive population modeling allows for an *a priori* assessment of the influence of

physiological properties on the pharmacokinetic behavior of drugs, prior to clinical studies.

In this study, the development of a physiology-based population model, which is linked to PK-Sim®, is described. The objective was to create a population of virtual individuals from *a priori* distributions of the relevant anthropometric parameters (i.e., distributions of the body dimensions), that is a reasonable representation of a real human population and further, to simulate drug concentration profiles in plasma as a measure of pharmacokinetic variability. A similar attempt to model inter-individual anthropometric variability has recently been described by Price *et al.* (9) based on the P^3M tool. Virtual individuals from this study will be compared to the individuals of this previously published model. Further, population PBPK simulations will be compared with experimental pharmacokinetic data for two model compounds, ciprofloxacin and paclitaxel. Although children are explicitly included in the population model as a sub-population, this paper focuses on adult data only. The details of the children PBPK model and a comparison between simulated and experimentally obtained plasma concentrations in children have been reported in a separate study (10).

METHODS

Background of the PBPK Model Used

All PBPK simulations were carried out using the software PK-Sim® Version 3.0 (2,7,8,10). In short, PK-Sim® is a generic PBPK-model with 17 organs and tissues. Each organ further consists of four sub-compartments namely the plasma, red blood cells (which together build the vascular space), interstitial space, and cellular space. As input parameters, physico-chemical properties (lipophilicity, plasma protein binding constant or alternatively fraction unbound in plasma, and molecular weight) as well as compound specific clearance information (either *in vivo* plasma or blood clearances or intrinsic clearances determined from *in vitro* experiments) are required. From the physico-chemical properties, the model parameters relevant for a PBPK simulation are estimated. In case of the organ/plasma partition coefficients, a physiological model is used which describes partitioning between the aqueous sub-compartment and the lipid and protein components in plasma and the respective tissue (11) using the known tissue composition (water, lipid and protein content) for each organ (12). For a detailed description of the underlying PBPK model and the input/output parameters of PK-Sim® refer to the user manual available at www.pk-sim.com.

Data Collection

PBPK simulations in realistic human individuals or populations require knowledge about mean values as well as variabilities and distributions, respectively, of relevant anthropometric parameters, primarily body weight (BW), height (H), and body mass index ($BMI = BW/H^2$). Valuable sources for this information were available in the NHANES III study (13) and the Annals of the ICRP (14). In the NHANES III study (13), the health and nutritional status of approximately 30 thousand individuals aged from 2 months to 90+ years and inclusive of different races were investigated. From this data set, age-, gender, and race-dependent anthropometric data were obtained. The individual data were pooled into 12 age groups ranging from 3 years to 70+ years. The NHANES III data set (13) provided sufficient information to derive statistically meaningful distribution curves for BW, H and BMI over the whole age range for Caucasian (referred to in the NHANES III data set as "white"), afro-American ("black") and white Mexican American populations. Information on other races from NHANES III (13) were not used since the number of study subjects was low [curves were considered statistically meaningful if every age group contained the data of at least 30 individuals (15)]. Cubic spline functions using the parameter values in the middle of each age range were used to generate continuous functions across the whole age range.

Information on mean organ weights (expressed either in absolute numbers or as fractions of body weight) and blood flows were gathered from the ICRP report (14). This reference provides only a mean adult value and is independent of age. Thus elderly individuals were not treated differently than younger adults. For simplicity reasons, a constant density of 1 g/ml was assumed for all tissues, in order for mass (in [g]) to be set equal to volume (in [ml]). All volumes were inclusive of the organ-specific blood volumes as derived from ICRP (14). The relative organ weights and blood flows for adults, as presented in Table I, were considered independent of race. Information on the variability and distribution functions of organ weights and blood flows among individuals was also gathered from the literature and is discussed in the 'Algorithm to Create a Virtual Population' section.

Algorithm to Create a Single Virtual Individual

A single virtual individual is created on the basis of the collected anthropometric data. Upon definition of the desired race, gender and age, the appropriate BW, H and BMI distributions are used. Based on the user input of the height-weight relation of the target individual, defined by

Table I. Absolute and Relative Organ Volumes (including blood content) and Blood Flows of the "Mean" Caucasian Male (BW = 73 kg, H = 176 cm, BMI = 23.6 kg/m^2) and Female (BW = 60 kg, H = 163 cm, BMI = 22.6 kg/m^2)

	Volumes				Blood Flow Rates			
	Male		Female		Male		Female	
Organ	V (ml)	% of BW	V (ml)	% of BW	Q (ml/min)	% of CO	Q (ml/min)	% of CO
Lung	1294	1.8	1009	1.7	6106	100	5504	100
Brain	1509	2.1	1357	2.3	780	12.8	708	13
Kidneys	438	0.60	403	0.67	1325	21.7	1121	20
Liver	2358	3.2	1905	3.2	423	6.9	383	7
Pancreas	190	0.26	169	0.28	65	1.1	59	1
Spleen	243	0.33	219	0.37	195	3.2	177	3
Stomach	168	0.23	163	0.27	65	1.1	59	1
Small Intestine	724	1.0	694	1.2	650	10.6	649	12
Large Intestine	412	0.56	417	0.69	260	4.3	295	5
Muscle	32339	44.3	20276	33.8	1106	18.1	665	12
Heart	417	0.57	328	0.55	260	4.3	295	5
Adipose	14868	20.4	19348	32.2	325	5.3	501	9
Bone	11818	16.2	9122	15.2	325	5.3	295	5
Skin	3761	5.2	2724	4.5	325	5.3	296	5
Gonads	40	0.06	13	0.02	3	0.05	1	0.02

Organ volumes not including their blood content were taken from ICRP (14).

setting two parameters out of body weight (BW_{target}), height (H_{target}), or body mass index (BMI_{target}), the organ volumes and blood flows are generated. This involves correlations to be developed for organ volumes and blood flows with BW, H and/or BMI.

The starting point for the creation of the target individual is always a "mean individual" of the gender at the given age (see Fig. 1). This mean individual exactly falls on the mean for body weight (BW_{mean}), height (H_{mean}), and body mass index (BMI_{mean}) for the given race, age and gender. At first, an intermediate individual is created with the height of the target individual, but a weight indexed to BMI_{mean}. This intermediate can be interpreted as an average sized individual with the target height, but not the target weight. Adjustment of the weight to the target weight includes both organ weight generation and fat addition, as described below.

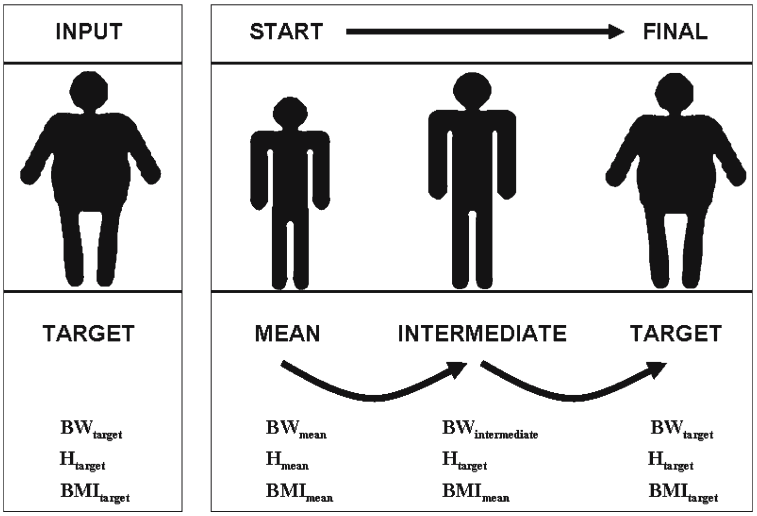

Fig. 1. Process for adjusting a single 'mean' virtual individual to a 'target' individual with a user-defined body weight (BW), height (H) and body mass index (BMI).

For the target individual, the organ weights (OW_{target}) are calculated from the mean organ weights (OW_{mean}, summarized in Table I) using an allometric scaling function with height,

$$OW_{target} = \left(\frac{H_{target}}{H_{mean}}\right)^{0.75} OW_{mean} \quad (1)$$

Scaling with body height is in accordance with findings of de la Grandmaison *et al.* (16) who investigated autopsy data for organ weights (heart, right and left lung, liver, spleen, pancreas, kidneys and thyroid gland) in 684 female and male adults. They demonstrated that the organ weights were better correlated with body height than with BMI or BW (16). Equation 1 is applied to all organs except brain, fat and skin tissue. The ICRP data reveals that the brain weight is largely independent of the body weight or height of a person for a given age and gender (14), and is, thus, kept constant ($OW(brain)_{target} \equiv OW(brain)_{mean}$). The weight of the fat tissue is calculated as the difference between the target body weight and the sum of all other organ weights of the intermediate individual. This procedure follows the assumption that overweightedness is caused by an increase of the fat tissue rather than muscle or other tissues. Thus, a high body mass index in this algorithm is always associated with obesity and, individuals with a comparatively higher body weight for a given height,

which is caused by a large muscle rather than fat content (such as athletes or body builders), are underrepresented. In case of the skin, application of Eq. 1 yields the skin weight of the intermediate individual from Fig. 1 rather then the target individual, because OW(skin) is proportional to BSA, which in turn, is proportional to BW with an exponent around 0.5 (17–20). Thus, an additional correction for the influence of over- or underweightness is required. To obtain the target skin weight ($OW(skin)_{target}$) the following equation is used:

$$OW(skin)_{target} = \left(\frac{BW_{target}}{BW_{intermediate}}\right)^{0.50} OW(skin)_{intermediate} \quad (2)$$

Organ blood flows are scaled to the total cardiac output (CO, is equal to the blood flow of the lung). Indexing cardiovascular variables to height is suggested as more appropriate than other indices (e.g., BSA) for both lean and obese individuals (21,22) and, thus, CO is scaled according to:

$$CO_{target} = \left(\frac{H_{target}}{H_{mean}}\right)^{0.75} CO_{mean} \quad (3)$$

The target organ blood flows are then calculated based on the constant relative fractions, as given in Table I, from CO_{target}.

The described algorithm was linked to the PBPK software tool PK-Sim® as a new module called "Create Individual". Upon definition of the input parameters for the target individual (race, gender, age, and two parameters out of BW, BH or BMI), the corresponding organ weights and blood flow rates are calculated automatically.

Algorithm to create a Virtual Population

The algorithm to create a population makes use of the algorithm to create a virtual individual, but also considers inter-individual variabilities of the anthropometric parameters. A flowchart of this algorithm ("PK-Pop") is presented in Fig. 2. To create a target population of n individuals, the race, age range, gender distribution (given as percentage females in the population), and the desired height/weight relationship (by defining minimum and maximum values for two parameters out of BW, H, and BMI) are input instead of single values as described above. First, each individual of the population is randomly assigned an age and gender according to the user-defined ranges and distributions. The "mean individual" for the assigned age and gender is created according to the single individual algorithm described above. Next, a new height is randomly assigned from

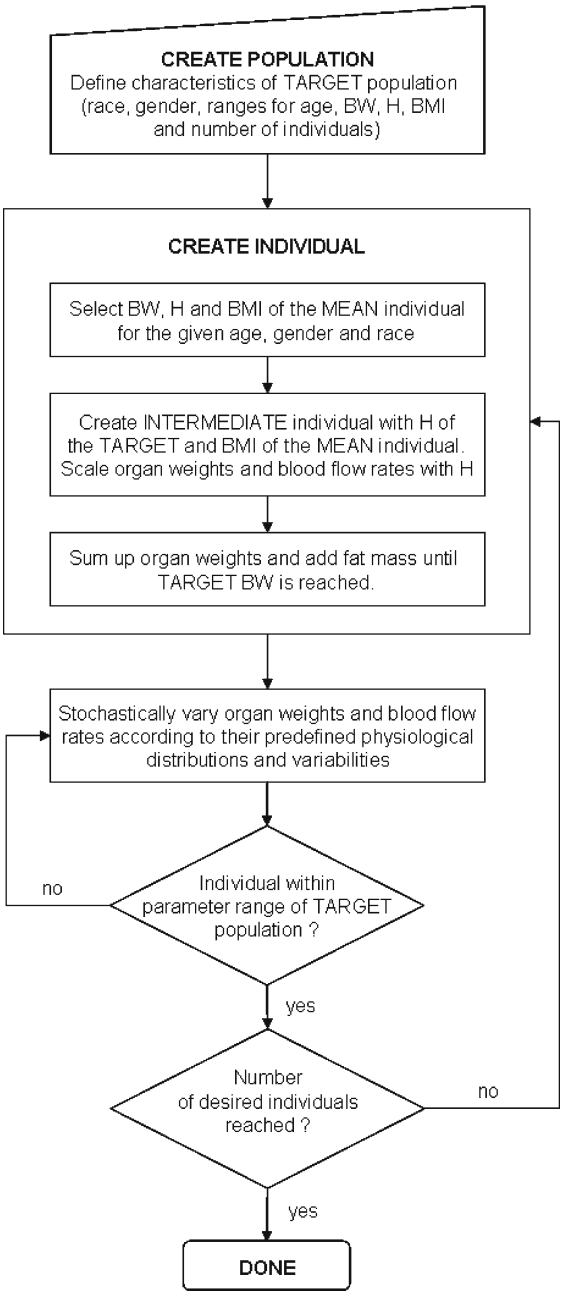

Fig. 2. Flow-chart representing the algorithm for the creation of a virtual population.

within a normal distribution (13) with the mean of the distribution equal to the height of the mean individual. Again, an intermediate individual is created keeping the same BMI as the mean individual. Then, new organ weights are generated as described above. In addition, each organ weight is randomly varied using predefined organ weight distributions by employing a Monte-Carlo method. Gaussian distribution functions are assumed for all organ weights except muscle, fat tissue (23), lung (16), and spleen (16), which are log-normally distributed. Only the variability within individuals of similar size must be considered here because the variability related to the different heights was already accounted via the scaling laws applied in Eqs. 1 and 3. Therefore, the literature was searched for information about the variability of organ weights for individuals with similar height. For the organs where only the total coefficient of variation (within a largely varying population) was reported (CV_{total}), as e.g., in the ICRP report (14), the relative body height variability (CV_{height}) was deduced from CV_{total} in order to obtain only the coefficient of variation for the organ weight (CV_{organ}) within individuals of similar height. Based on the scaling law in Eq. 1, CV_{organ} was calculated from:

$$CV_{organ} = \sqrt{CV_{total}^2 - (0.75\, CV_{height})^2} \tag{4}$$

Each individual parameter is assigned a coefficient of variation derived from literature sources (13,14,16,24–28) as a measure of inter-individual variability. In general, this variability can be age-, gender-, and race-dependent, but only very little race-specific information was available (none of this was used). The resulting coefficients of variation for the organs for adults are shown in Fig. 3. Their values vary between approximately 1% for the bone and 45% for the skin. Muscle weight has a geometric standard deviation of 1.1 in all races and is independent of gender. For fat tissue, the geometric standard deviations were race-specific and varied between 1.5 and 1.65 in females, and between 1.5 and 1.7 in males. These log-normal variabilities in muscle and fat content mainly contributed to the overall log-normal distribution of BW and BMI in a realistic population (13).

After the stochastic variation of the intermediate organ weights, the resulting body weight is calculated as the sum of the individual organ weights. The individual is then checked whether it fulfills the predefined BW and BMI criteria of the target population. If so, the individual is added to the virtual population, if not, it is withdrawn. Contrary to the creation of a single virtual individual, the stochastic nature of the population algorithm allows for the attribution of any weight above that of an average sized individual to fat *and* muscle, rather than solely to fat.

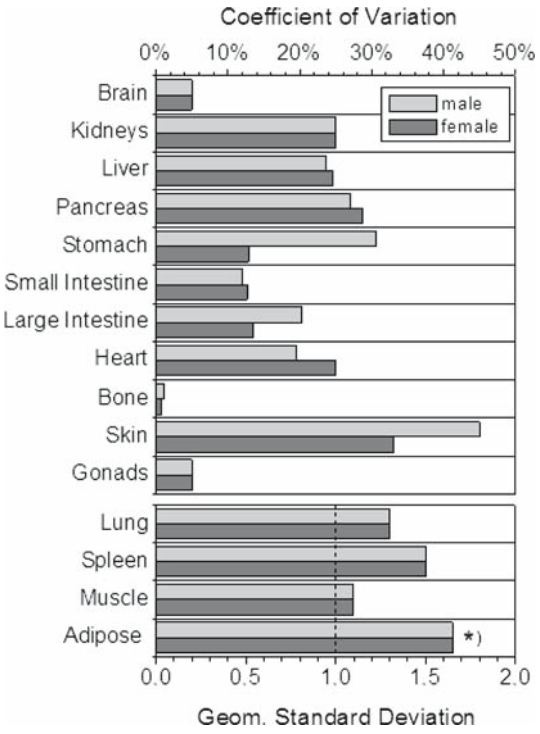

Fig. 3. Gender-dependent relative coefficients of variation for normally distributed organ weights and geometric standard deviations for log-normally distributed organ weights (the dotted line indicates a geometric standard deviation of 1, which equals no variation), *): race-specific, see text.

Because the geometric standard deviation in fat is larger than in muscle tissue, it is more likely that an obese individual is created than an individual with high muscle and low fat content.

As in case of the virtual individuals described above, the organ blood flows are calculated from the cardiac output, which is allometrically scaled with height, for each individual accepted into the population. Additionally, each organ blood flow is stochastically varied according to a normal distribution. Very little literature information about the inter-individual variability of organ blood flows was available. As a reasonable estimate, we assume a relative standard deviation of 5% for all organs (within individuals of the same height). The sign of the variation is kept the same in all organs, which lead to blood flows of the target individual that are all either above or below the intermediate blood flows. This consideration ensures that a higher or lower cardiac output affects all organs in the

same direction, which is reasonable because all organs are linked via the systemic circulation. Similarly to the final body weight, the final cardiac output is then re-calculated as the sum of all organ blood flows.

Consistency Check of Anthropometric Parameters with the NHANES III Data Set

Using the PK-Pop algorithm to create virtual populations for all ages, both sexes and the three races, the resulting anthropometric measures of BW, H and BMI were superimposed onto the BW, H and BMI distributions from NHANES III (13). The goal was to ensure that the algorithm produced realistic populations in terms of these parameters by comparing the 95% percentiles of the target population with the NHANES III data (13). For each gender and race, eight thousand individuals, uniformly distributed in the age range between 3 and 80 years, were generated. No limits were given for the BW, H and BMI for any of the simulations.

Comparison of Virtual Populations Created with PK-Pop and P^3M

Two thousand male and two thousand female virtual individuals from the three races in the age range of 25–35 years were created and their anthropometric parameters (BW, H, and BMI) as well as organ volumes and blood flows were compared to the results obtained with the P^3M tool, as reported in Price *et al.* (9). Correlation coefficients for the mean organ weights and blood flows generated using our model and the P^3M model were calculated.

As an independent check for consistency of the generated data, total adiposity (g of adipose tissue) and variability from the generated white male and female virtual populations were compared to literature data from a cadaver dissection study (29).

Comparison with Experimental Data

As a proof of concept, we compared simulation results for different virtual populations with experimental data obtained in clinical studies. As examples, two model drugs, ciprofloxacin and paclitaxel, were investigated. Ciprofloxacin is a widely used anti-infective. It is a small, hydrophilic molecule with a molecular weight of 331.4 and a lipophilicity of LogMA = 0.95 [logMA denotes the logarithm of the membrane affinity, i.e., a partition coefficient between water and an immobilized lipid bilayer (30)]. Paclitaxel is a taxane derivative that has antitumor activity against malignancies of the lung, breast, ovaries, head and neck (31). Paclitaxel is

Table II. Compound Related Properties of Ciprofloxacin and Paclitaxel Used in the Pharmacokinetic Simulations

Property	Ciprofloxacin	Paclitaxel
Lipophilicity (log units)	0.95	3.3
Molecular weight (g/mol)	331.4	858.9
Plasma Fraction Unbound	67%	8% (4–8%)[a]
Total Clearance (ml/min/kg)	7.0	5.5

[a]Randomized under a uniform distribution from 4% to 8% in simulation (B2)

a comparatively large molecule (molecular weight of 858.9) with a medium lipophilicity of 3.3 (log units). The compound specific properties of the two drugs used as input for the simulations are summarized in Table II.

The endpoint was the assessment of the variability in plasma concentrations and pharmacokinetic parameters due to inter-individual variations in the volume of distribution and clearance in the virtual compared to the real population. In addition to the effect of organ weights and blood flow parameters on compound pharmacokinetics, the inter-individual variability of clearance is an important factor. To assess the influence of inter-individual variability in clearance separately from the influence of anthropometric variability, three sets of PK-Pop simulations were performed for each test compound. In the first simulation, a population of anthropometrically different individuals ($n = 100$) was created. Regarding clearance, all individuals in this population were assumed to have the same intrinsic clearance per gram of tissue (population "A"). This was achieved by first separating the total blood clearance into renal, hepatic, and biliary contributions and then converting these blood clearances (CL_{bld}) into intrinsic clearance values (CL_{int}) using the well-stirred model equation:

$$CL_{int} = CL_{bld} \frac{Q}{Q - CL_{pls}} \cdot \frac{1}{f_{uB}} \tag{5}$$

Here Q represents the blood flow of the eliminating organ (kidney or liver), and f_{uB} is the fraction unbound in blood. Thus, simulation "A" only reflects the variability originating from anthropometric differences of the individuals. To assess the pharmacokinetic variability originating from inter-individual differences in the clearance, an additional virtual population ($n = 100$) was generated where all individuals had the same age, gender, weight and height but with clearance variation (population "B1") and in case of Paclitaxel an additional fraction unbound variation (see below, population "B2"). The total influence of anthropometric plus inter-individual variability in intrinsic clearance was finally studied in a virtual

population which combined both sources of pharmacokinetic variability (population "C").

In the ciprofloxacin study, a 400 mg dose of the drug was administered intravenously as a 60-minute infusion (32). Two-thirds of the mean ciprofloxacin clearance in adults of 7.0 ml/min/kg (31, 32) is due to renal elimination via both glomerular filtration and tubular secretion (33, 34). The remaining clearance is due to biliary and/or intestinal secretion (16%) (34) and via Phase I metabolism, primarily via the CYP450 enzyme, CYP1A2 (14%) (33, 35). Metabolic clearances of probe substrates for this enzyme and compounds that are primary secreted via the kidney tubules showed a relative inter-individual variability of 42% (36) and 22% (37), respectively. Consequently, clearance due to CYP1A2 and tubular secretion were statistically varied in simulation "B1" assuming a log normal distribution by these percentages in the population simulation. Because all individuals in the clinical study had normal creatinine clearance (>90 ml/min/1.73 m^2), the intrinsic clearance per gram kidney weight due to the passive process of glomerular filtration was kept constant for all virtual individuals. Similarly, for biliary secretion, the intrinsic clearance per gram liver weight was also kept constant in both simulations "A" and "B". To correspond to the experimental study population, a virtual male population with an age range of 35–55 years, a weight range of 63–112 kg and a height range of 165–188 cm was created. These weight and height ranges corresponded to the 95th percentiles for a 45-year-old man as reported in the NHANES III study (13).

For paclitaxel, four plasma concentration time data sets (38–40) were used where the drug was administered as a 3-hour intravenous infusion. Paclitaxel is administered based on mg/m^2. To convert the body-surface area related dose to the body weight related dose (as required by PK-Sim® as input), we used the formula of DuBois and DuBois (17). A population consisting of fifty female and fifty male virtual individuals with an age range of 35–75 years, a weight range of 50 to 112 kg and a height range of 152–188 cm was created, and pharmacokinetic simulations were subsequently performed. The weight and height range corresponded to the 95th percentile for 50 year old men and the 5th percentile for 50 year old women, according to the NHANES III data (13). The clearance of paclitaxel is about 5.5 ml/min/kg in adults. Primary routes of elimination are via the hepatic enzymes CYP2C8 and CYP3A and only 5% is renally cleared (31). Inter-individual metabolic clearance variabilities are 50% for both CYP2C8 (41) and CYP3A (42). Accordingly, these clearances were randomized in simulation "B1" and "B2" assuming a log normal distribution. Furthermore, paclitaxel is highly bound to plasma proteins (92%) and is formulated in a matrix that can decrease the unbound fraction in plasma

to 4% (39). To account for this effect in the simulations, the fraction unbound of paclitaxel was statistically varied in simulation "B2" assuming a uniform distribution between 4 and 8%.

The coefficients of variation of the pharmacokinetic parameters, volume of distribution at steady state (Vss), clearance (CL) and area under the plasma concentration time curve (AUC), obtained in these simulations were compared to CVs obtained in the corresponding clinical studies.

RESULTS

Comparison of Anthropometric Parameters with the NHANES III Data Set

Figure 4 presents the distributions of BW, H, and BMI for males of a north-American Caucasian population. The NHANES III (13) data is shown as 5% to 95% percentile lines. Virtual individuals from the generated population are shown as symbols. Over the whole age range for all races and both genders, 89.2, 92.0, 89.7% of the generated virtual individuals were within the 5% to 95% percentile interval of the NHANES III data for BW, H and BMI, respectively. These values correspond well to the theoretically ideal value of 90%. There was a slight upwards bias in BW and subsequently also BMI. For the whole data set, 5.8% of the individual BWs were above the 95th percentile and 2.2% were below the 5th percentile.

Comparison of Virtual Populations Created with PK-Pop and P^3M

Table III summarizes the results of the comparison between PK-Pop and P^3M. Overall, high correlation coefficients between the corresponding mean values were obtained. For the observed mean organ volumes, the correlation coefficients are 0.983 (males) and 0.990 (females), with slopes of 1.071 (males) and 1.095 (females), indicating a very good agreement. Remarkable differences between the PK-Pop and the P^3M model exist in the coefficients of variation of the log-normally distributed organ volumes. While the CVs of lung, spleen, and fat are greater in the PK-Pop than in the P^3M model, the distribution of muscle weight is smaller in PK-Pop. Another remarkable difference is the variability of bone weight. In the P^3M model, the CV for the bone is more than two times greater than the value from PK-Pop. For the blood flows, correlation coefficients of 0.996 (males) and 0.989 (females) and slopes of 0.842 (males) and 0.781 (females) were obtained. This indicates a good correlation with a systematic deviation in the absolute values between the two models. The CVs of the blood flows were in general agreement, with substantial differ-

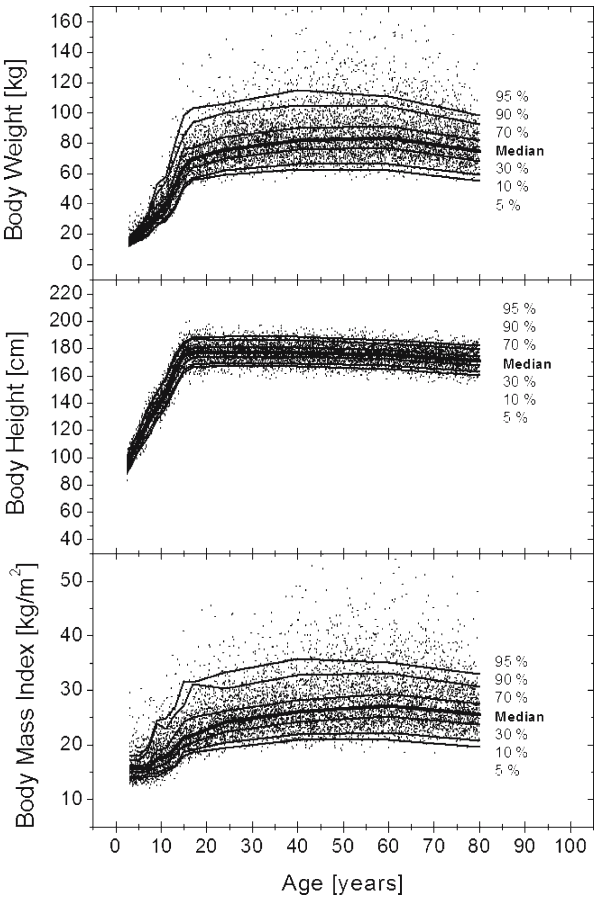

Fig. 4. Body weight, body height and body mass index as a function of age for a north American male population. Lines represent percentiles from the NHANES III database (13). Symbols represent 8000 virtual individuals per graph as generated in PK-Pop.

ences seen in spleen and fat tissue. Total adipose tissue, as estimated in PK-Pop, was (±SD) $15,792 \pm 6,536$ g [range 4,223–48,850] in the white male virtual population and $20,464 \pm 8,216$ g [range 5,507–59,257] in the white female virtual population.

Comparison with Experimental Pharmacokinetic Data

Table IV presents the results of simulations where the anthropometric input parameters as well as, clearance and/or fraction unbound were

Table III. Comparison of Arithmetic Means, Standard Deviations, and Coefficients of Variation for Anthropometric Parameters, Organ Volumes, and Blood Flows in Virtual Populations Created with P^3M (X) (9) and PK-Pop (Y)

		Adult-males (25–35, all ethnic groups, $N = 2000$)						Adult-females (25–35, all ethnic groups, $N = 2000$)					
		P^3M			PK-Pop			P^3M			PK-Pop		
		Mean (X)	Std. Dev.	CV	Mean (Y)	Std. Dev.	CV	Mean (X)	Std. Dev.	CV	Mean (Y)	Std. Dev.	CV
Antropometry													
Body Weight	(kg)	83.1	17.9	0.22	80.4	13.5	0.17	68.9	17.2	0.26	68.8	15.5	0.23
Height	(cm)	176.5	7.5	0.04	174.4	7.6	0.04	162.9	6.5	0.04	161.7	6.9	0.04
Body Mass Index	(kg/m^2)	26.7	6.06	0.23	26.4	4.1	0.15	26.0	6.91	0.27	26.3	5.8	0.22
Volumes													
Lung	(ml)	1010	130	0.13	1326	359	0.27	870	120	0.14	1057	289	0.27
Brain	(ml)	1340	80	0.06	1508	74	0.05	1200	80	0.06	1354	67	0.05
Kidneys	(ml)	320	68	0.22	444	110	0.25	260	68	0.26	413	106	0.26
Liver	(ml)	1570	260	0.16	2341	560	0.24	1350	270	0.2	1938	490	0.25
Pancreas	(ml)	100	18	0.18	190	52	0.27	86	17	0.2	174	50	0.29
Spleen	(ml)	220	37	0.17	269	110	0.41	190	38	0.2	247	105	0.43
GI organs	(ml)	1230	220	0.18	1312	143	0.11	1170	230	0.2	1306	135	0.10
Muscle	(ml)	32000	5600	0.18	32514	3635	0.11	21000	4130	0.2	20972	2384	0.11
Heart	(ml)	360	51	0.14	418	85	0.20	300	42	0.14	336	88	0.26
Adipose	(ml)	28690	11840	0.41	21946	12289	0.56	31270	13160	0.42	26928	14859	0.55
Bone	(ml)	9220	1570	0.17	11820	786	0.07	6100	1160	0.19	9379	634	0.07
Skin	(ml)	3870	449	0.12	3800	392	0.10	3340	449	0.13	2824	358	0.13
Gonads	(ml)	–	–	–	39.9	3.5	0.09	–	–	–	13.4	1.2	0.09
Correlation of means					$Y = 1.071*X - 289 (R = 0.983)$						$Y = 1.095*X - 513 (R = 0.990)$		

Table III. continued

Blood Flow Rates													
Cardiac Output	(ml/min)	5450	740	0.14	6293	809	0.13	4680	720	0.15	5781	725	0.13
Brain	(ml/min)	680	0	0	778	70	0.09	630	0	0	707	63	0.09
Kidneys	(ml/min)	1170	250	0.22	1356	372	0.27	850	22	0.26	1150	323	0.28
Liver	(ml/min)	1320	220	0.16	1689	269	0.16	1350	270	20	1687	261	0.15
Pancreas	(ml/min)	60	11	0.18	65.3	19.3	0.30	50	10	0.2	60.8	18.8	0.31
Spleen	(ml/min)	220	40	0.17	216	91	0.42	100	40	0.2	200	88	0.44
GI organs	(ml/min)	930	160	0.18	1266	203	0.16	910	180	0.2	1294	204	0.16
Muscle	(ml/min)	950	170	0.18	1115	178	0.16	630	120	0.2	692	110	0.16
Heart	(ml/min)	730	0	0	778	70	0.09	960	0	0	707	63	0.09
Adipose	(ml/min)	570	240	0.41	429	81	0.19	940	390	0.42	629	130	0.21
Bone	(ml/min)	590	100	0.17	327	43	0.13	390	74	0.19	304	39	0.13
Skin	(ml/min)	470	54	0.12	332	50	0.15	510	68	0.13	309	50	0.16
Gonads	(ml/min)	–	–	–	3.3	0.5	0.14	–	–	–	1.2	0.2	0.14
Correlation of means			$Y = 0.842 * X + 67$ $(R = 0.996)$							$Y = 0.781 * X + 120$ $(R = 0.989)$			

Table IV. Observed and Simulated Coefficients of Variation for Ciprofloxacin and Paclitaxel Pharmacokinetic Parameters

		Input Parameter Varied				
		Physiology	Clearance	Clearance and fu	Physiology, Clearance and/or fu	
Compound	Population Pharmacokinetic Parameter	"A" [CV]	"B1" [CV]	"B2" [CV]	"C" [CV]	[CV] (experiment)
Ciprofloxacin[a]	Vss	7%	5%	–	7%	10%
	CL	15%	14%	–	16%	20%
	AUC_{end}	11%	14%	–	13%	14%
Paclitaxel[b]	Vss	9%	3%	17%	19%	n.d.
	CL	13%	15%	19%	25%	26%
	AUC_{end}	14%	15%	19%	25%	28%

[a]Geometric coefficient of variation. Observed data from Shah *et al.* (32).
[b]Arithmetic coefficient of variation. Observed data from Panday *et al.* (38); no comparable data was available for Callies *et al.* (40).

varied singly or in tandem. For both test compounds, variability of Vss, CL and AUC were similar when either the anthropometry ("A") or the clearance was singly varied ("B1"). The CV of CL and AUC for paclitaxel appears to be heavily influenced by fu variation ("B2"). Interestingly, the CVs for Vss, CL and AUC following anthropometric and clearance variation were not additive, as is evident from the CV values obtained for populations "C". For ciprofloxacin, the addition of intrinsic clearance variability only slightly increased the CV of CL (+1%) and AUC (+2%) in comparison to a simulated population all having equivalent intrinsic clearance per gram of tissue weight. In the case of paclitaxel, the addition of clearance and fraction unbound variability increased the CV of the Vss (+10%), CL (+12%) and AUC (+11%) in comparison to the simulated population where the individuals all had equivalent intrinsic clearances and identical fraction unbound.

Plasma concentration time curves resulting from the population simulations "A" and "C" are presented in Fig. 5(A) and (B) for ciprofloxacin together with the experimental study data (32). Both, the mean and the variability in the observed concentrations are well represented by the generated population concentration time curves (Fig. 5). For paclitaxel (Fig. 6), all concentration-time curves are shown dose normalized to allow for a better comparison. The curve shape is accurately simulated although the variability during the infusion phase is underestimated. The remainder of the points before and after the C_{max} are however, well represented.

DISCUSSION

Several attempts to include the aspect of inter-individual variability into PBPK models using stochastic methods have been described in the literature, mostly in the framework of toxicological risk assessment (43–51). Jonnson *et al.*, for example, used PBPK models where mean physiological parameters were linked to covariates such as body weight and height, lean body mass, etc. by scaling laws (44–46). Using a Bayesian approach with Markov-chain Monte-Carlo simulations, the inter-individual variability in the physiological parameters was then assessed by fitting the outcome of the PBPK model to experimental toxicokinetic data derived in a number of individuals (44–46). A drawback of this method is that the resulting coefficients of variations for organ volumes and blood flow rates depend on uncertainties resulting from analytical procedures and are, furthermore, sensitive to potential model-misspecifications, since they were derived from a fit to experimental data. Another limitation of the population models developed for toxicokinetic applications is that they are often not fully physiology-based. Instead, it is very common to simplify the physiology of the organism by "lumping" certain organs together. One commonly used lumping scenario is based on perfusion, where compartments are lumped into "slowly" and "rapidly perfused tissues" (43–46,48,49). This simplification is justified in cases of small compounds, which predominately exhibit perfusion-limited kinetics. But most compounds that are of interest in pharmaceutical drug development have relatively large molecular weights (several hundred daltons) and can become permeation-limited in some of the organs, which prohibits the lumping of organs on the basis of their blood-flow rates. This fact limits the applicability of blood-flow limited PBPK models in drug research and discovery. In terms of the assessment of inter-individual variability, the above mentioned PBPK models do not deliver information about physiological variability in the organs that are lumped together. Very recently, Gueorguieva *et al.* (52) presented a Bayesian population model for diazepam that combines a whole body-PBPK model with distributions of physiological parameters derived from experimental pharmacokinetic data.

In the present study, it was the goal to develop a whole-body PBPK model with inter-individual variability based on *a priori* knowledge of anthropometric distributions. It is essential to know and account for these full multivariate distributions, and understand the cross correlations involved. The most comprehensive comparable approach has so far been

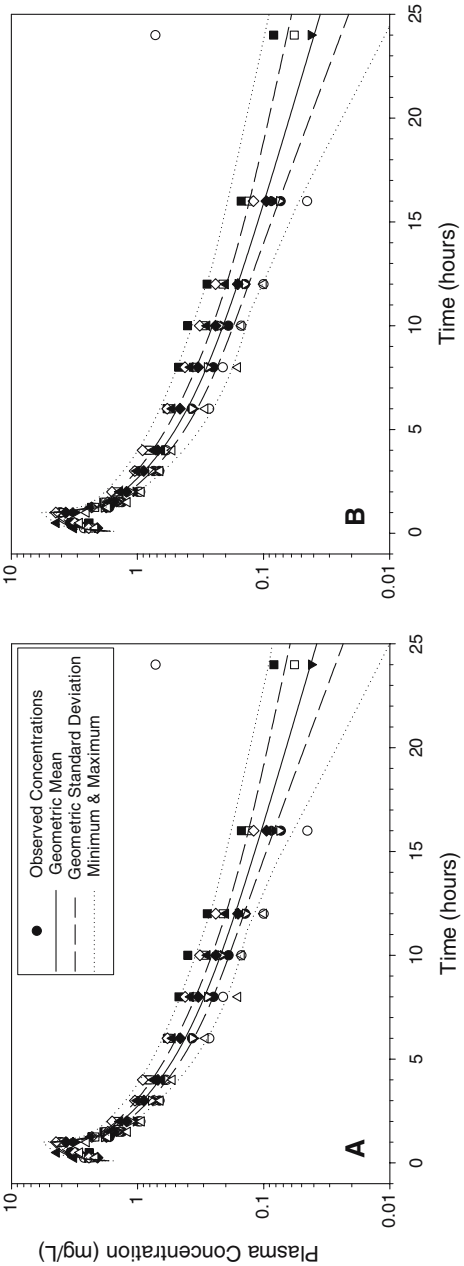

Fig. 5. Predicted (lines) and observed (symbols) individual ciprofloxacin plasma concentrations following an intravenous administration of 400 mg as a 1-hour infusion (32). In graph A, only anthropometric and physiological parameters were varied in the virtual population (population "A"). In graph B, additional inter-individual variation of active clearance processes were regarded (population "C").

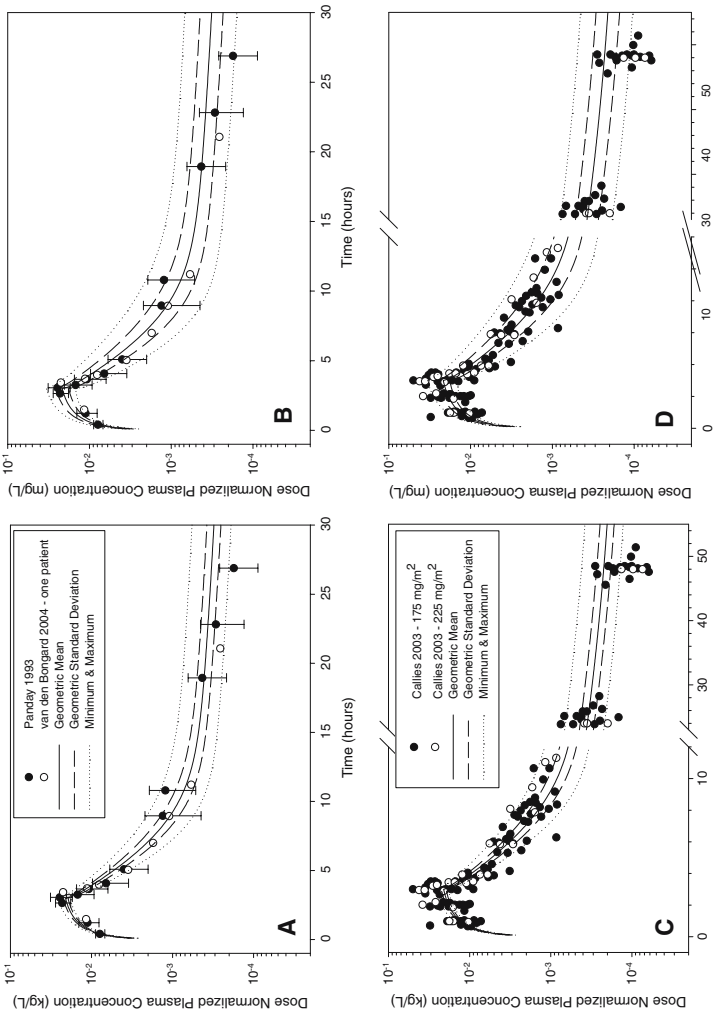

Fig. 6. Dose-normalized predicted (lines) and observed mean ± standard deviation (38) or individual (39,40) plasma concentrations (symbols) of paclitaxel following an intravenous administration of 175 mg/m^2 or 225 mg/m^2 as a three-hour infusion. In graph A and C, only anthropometric and physiological parameters were varied in the virtual population (population "A"). In graph B and D, additional inter-individual variation of active clearance processes and fraction unbound were regarded (population "C").

presented by Price *et al.* (9). Despite the close association of organ weights and blood flows obtained from our model to those proposed by Price *et al.* (9) (Table III), the methods used to generate these values were different. We describe the creation of single virtual individuals according to a pre-defined height/weight relation in combination with the definition of gender, age, and race. The cross correlations between organ weights, blood flow rates and anthropometric parameters are regarded by means of scaling laws (Eqs. 1–3). More in depth data, such as simultaneous individual organ weight measurements along with their respective blood flows in a diverse population, would supersede the use of these scaling laws; however this type of information is not available in the literature. In our model, the individual organ weights and blood flows are calculated based on reported relative fractions from the body weight and cardiac output, respectively. These fractions were found to be gender specific (Table I), and in case of the weight of the fat tissue, also race-specific. No race-specific information about relative blood flows was available to us at the time of model development. Nevertheless, the underlying data structure in the model allows for the definition of race-dependent organ volume and blood flow fractions, in case this information becomes available in the future. It should be emphasized that no stochastic process is involved in this algorithm for the creation of a single virtual individual.

A virtual population is defined by ranges for age, weight and height in addition to the gender and race. Then, the algorithm to create a single virtual individual is combined with a stochastic Monte-Carlo method, which makes use of predefined variabilities and distribution functions of organ weights and blood flows. As a result, a population is created within the user defined ranges, which, for the parameters of BW, H and BMI, is mostly consistent with the NHANES III data (13). The slight upwards bias in BW is due to the stochastic addition of excess BW to fat and muscle mass. For these tissues, log-normal weight distributions are assumed, which tend to slightly overestimate the excess organ weights in underweight individuals.

In contrast, Price *et al.* (9) generated a database of values by employing literature based predictive equations referenced to age, gender, race and anthropometric parameters, to generate mean values for organ weights and blood flows across the age range of the NHANES III study (13). Inter-individual variation for these values is generated retrospectively by randomly selecting individuals from the NHANES database (13), generating the predicted organ weights and blood flows from the predictive equations and calculating the arithmetic mean of each parameter for the population. In our study, the inter-individual variability and distribution of each organ weight and blood flow is provided *a priori* and assigned to

the individuals of the population via a Monte Carlo method. Inter-individual variabilities of organ weights and blood flows, which are caused by differences in body height or body weight, are already accounted for via scaling laws. But even among individuals of similar stature, inter-individual differences remain. To account for those, organ specific coefficients of variation have been derived via Eq. 4. Regardless of the method used, the mean weights and blood flows are highly correlated. In the case of blood flows, there is a systematic deviation between the two models. On average, the blood flows used in this model are 16% (males) and 22% (females) larger than the values used in P^3M. Blood flows from both models, however, were derived from literature based values, and are considered reasonable.

For the variabilities, an external check is difficult for either model due to a lack of literature information on inter-individual variabilities of organ weights and/or blood flows within the anthropometric range of the individuals examined. Because adiposity is an important moderator of pharmacokinetics for some drugs (53), the adiposity of the virtual populations were checked against literature data obtained from a cadaver study. While this report represents one of the only that directly measures fat mass, the population examined was different from our virtual population. Cadavers ($n = 34$) were older (16–94 years; mostly above 55 years) and primarily selected based on "normal appearance" (29). Total mean adipose mass in the male and female cadavers were similar to the mean weight calculated using this model. The experimental values were 82% and 103% of the respective values of the virtual reference population. Coefficients of variation of adipose mass reported in this study for the male (54%) and female (48%) cadavers (29) were similar to those of the male (41%) and female (40%) virtual population. Despite the assumed anthropometric differences between the two populations, the mean adipose tissue mass and variability appears to be well predicted by the population algorithm.

The Price *et al.* (9) method assumes a normal distribution for all values, which is not consistent with the literature. In comparison, the CVs, especially in the case of the log-normally distributed organs, tended to be lower than those of the PK-Pop model, because the normal distribution in the Price *et al.* (9) model masks any extreme values observed in a real population. Another remarkable difference was seen in the inter-individual variability of bone weight. In the virtual population of Price *et al.* (9), the CV for bone is 17% and, thus, comparable to the CV of BW (22%). In PK-Pop, the CV for bone (7%) is much smaller and similar to the CV of height (4%). This seems to be more reasonable because overweightedness is unlikely to increase the mass of the skeleton. The ICRP report provides evidence that the bone mass variability in males and females is

at or below 10% (14). Both models predicted relatively large variabilities for spleen volume and blood flow. This finding may be explained since an enlarged spleen can become a chronic symptom following infection or disease (54, 55).

The blood flows in the P^3M model are calculated from perfusion rates normalized to the organ volume (9). As a consequence, the CVs of volume and blood flow are the same for every organ (with the exceptions of brain and heart, see Table III). In case of fat tissue, this approach is questionable. In obese people, either the size (in case of *hypertrophic adiposity*) or the number (*hyperplastic adiposity*) of adipocytes is increased together with the extent of adipose tissue microvasculature (56). But there is evidence, that the weight (57) or fat (58) normalized total blood flow in fat is smaller in obese individuals than in normal weight individuals. Our algorithm does not produce the same broad distribution for the blood flow as for the fat weight and is, thus, in accordance with this finding.

In summary, the presented approach is in accordance with published data for the means, distributions and variabilities of anthropometric parameters. This approach ensures that realistic virtual representatives of real individuals are created. In comparison to the other published model of Price *et al.* (9), we believe that our method for determining organ weight and blood flow variabilities and distributions is more inline with the literature.

Further, the relation between the variability within a virtual population and the pharmacokinetic outcome was evaluated. This evaluation was performed using two model compounds with different physico-chemical properties. Ciprofloxacin is a small molecule with low lipophilicity, whereas paclitaxel is comparatively large and has a greater lipophilicity. These compounds were selected for the evaluation (i) because of the availability of suitable experimental data and (ii) because of their quite different physico-chemical properties, from which it can be expected, that they exhibit different pharmacokinetic distribution properties. The mean plasma profiles of both compounds were, in general, very well described by the pharmacokinetic simulations. Only in the last sample time point for paclitaxel did the mean curve not follow the observed data. We assigned a constant fraction unbound to each virtual individual in the population; however, due to the formulation additive, the fraction unbound increases as the additive is eliminated (40). An increased unbound fraction leads to a greater distribution volume and higher apparent clearance thus lowering the blood concentrations, a process for which we did not account and which subsequently led to our overestimation of the plasma concentrations in the last time point.

Clearance is an important source of inter-individual pharmacokinetic variability. By default, the intrinsic clearance per gram of eliminating organ tissue is kept constant in PK-Pop. This is the most reasonable assumption in the case of renal and biliary elimination, because these physiological processes are proportional to the kidney and liver weight, respectively (under non-pathological conditions). The activity of metabolization processes in the liver however, also depends on the inter-individual expression of the respective enzyme, which can vary among different individuals. Clearance is related to age, for example, in case of enzymatic elimination processes in the liver, where the enzyme activity increases in early childhood (59), and decreases in elderly people (60). Also, certain race-specific differences in enzyme activity are well documented (61). But even individuals of the same gender, age, and race can show significant differences in the elimination of drugs due to, for example, polymorphisms in metabolizing enzymes (such as CYP2D6) or in active transporters, which are involved in the elimination process.

In the present study, the clearance variability was not predicted *a priori*. Instead, coefficients of variations determined in *in vivo* studies were used. The addition of intrinsic clearance variability with anthropometric variability in this study led to an increase in the predicted variability, although the influence was lower than expected. A sensitivity analysis demonstrated that anthropometric differences between individuals were equally as powerful in influencing the pharmacokinetic curves as was clearance variability, but the combined effects were not additive (Table IV) for the two model compounds. This is because the stochastically varied intrinsic clearances per gram tissue weight were randomly assigned to each individual, which masks some of the influence of physiological differences on the pharmacokinetics among individuals, and vice versa. The random allocation of intrinsic clearance was done because there was no information available regarding any cross-correlations of intrinsic clearance with anthropometric parameters in the populations that were studied. Cross-correlations of obesity in relation to plasma clearance and unbound fraction have been reviewed for several drug classes (43). The author of this study concluded that there is no systematic correlation of hepatic enzymatic activity, renal function or plasma protein binding to the extent of obesity, even though trends can be observed for some compounds (53).

The "Create Individual" algorithm always reproducibly generates identical virtual individuals when the input settings are identical, because of the lack of a stochastic process. This algorithm is particularly helpful when the sensitivity of the pharmacokinetic behavior with respect to a single physiological parameter is investigated. For example, a normal-weight individual can easily be compared with an obese virtual individual. In the

case of predictive population modeling, pharmacokinetic variability due to physiology can be assessed either with or without an additional variation due to parameters such as clearance, hematocrit and/or protein binding. As an example, differences in the unbound fraction in plasma can be treated. Such differences can be due to an inter-individually varying content of plasma proteins such as albumin or α-glycoprotein, or, as in case of paclitaxel, be caused by specific formulations. By including a stochastic allocation within a user-defined range and distribution, the effects of inter-individual variability on pharmacokinetics can be addressed.

This study focused on building a virtual population consisting of realistic representatives of a real population and further evaluating the pharmacokinetic variability obtained by this model with two compounds following intravenous administration. Because the collected anthropometric parameters mainly reflect the values of healthy individuals, the virtual individuals mainly represent healthy volunteers as studied in clinical phase I rather than real patient populations. In patient populations, several pathological conditions can occur which alter the physiology and, thus, the pharmacokinetic behavior of a drug compared to healthy individuals. Among those alterations are impaired functions of the eliminating organs, which affect the clearance of a drug and eventually require dose adjustments in these subpopulations. Other pathological conditions, such as e.g., malnutrition or a fatty liver, can indeed lead to additional variability in drug distribution due to changes in the body and/or tissue composition. Such pathological conditions are not represented in the underlying physiological database. The variability of distribution volumes observed using this model therefore only account for the inter-individual variations of the *body* composition in a healthy population by means of individually varying organ weights, but does not reflect potential differences in the *organ* composition (i.e., water, lipid and protein content) between individuals. An additional variation of the protein, water and adipose contents of each organ would lead to an increased variability in the distribution volume. In children however, the age-related interplay of fat and water in adipose tissue, and protein and water in muscle tissue, is known, thus leading to age-dependent distribution volumes as described in Edginton *et al.* (10). It should therefore be kept in mind that further adjustments of the physiological model parameters may be needed, when real patient populations are considered. PK-Sim® offers the option to manually adjust the generated 'normal individual' physiological parameters, but it remains a future goal to include relevant pathological conditions into the physiological database.

A second limitation of the presented model is the route of administration. While oral administration is usually preferred for most drugs, this

study only addressed the intravenous route, thus separating the variability in distribution and elimination from the variability of absorption. Absorption is, in addition, affected by physiological variables of gastric empting, intestinal transit time patterns, individual pH profiles and/or effective surface area available for absorption. Further, formulation effects are, in turn, affected by the individual gastrointestinal physiology (e.g., disintegration and dissolution of solid dosage forms). Physiology-based modeling of inter-individual variability following oral administration and absorption is the subject of ongoing work.

The advantage of PBPK population pharmacokinetics compared to the population pharmacokinetics approach is that single individual and population models can be used *a priori* to make predictions of pharmacokinetic profiles in humans prior to first-in-man studies. Since at this stage, no human *in vivo* clearance measure, a necessary input for any pharmacokinetic model, is available, extrapolations from animals or in vitro tests are required. Estimated inter-individual clearance variability can be determined from an understanding of the pathways of clearance and their in vitro variabilities or distributions (in the case of bimodel enzymatic activities, e.g., slow and fast metabolizers), as was demonstrated for ciprofloxacin and paclitaxel. Following first-in-man studies, the pharmacokinetic variability is more widely understood in a healthy population and can be extrapolated to a patient group or sub-population. These may include the elderly, children, obese and/or hepatically or renally impaired individuals. The effect of physiological changes, clearance cross-correlations or other anomalies can be simulated and the effect on pharmacokinetic variability assessed. This extrapolation is not possible in the classical population approach, unless the sub-population was included in the model, since the underlying model is based on compartmental kinetics and is not physiology-based. During the drug development process, a step-by-step inclusion of knowledge into the model during clinical development increases the accuracy of the output and confidence in the results. For instance, the known pharmacokinetic variability from the Phase 1 and II trials can be incorporated into the model prior to a large population simulation that would be required for a Phase III trial. This allows for hypothesis generation and testing to retrospectively understand the observed variability and its source (e.g., anthropometry or intrinsic clearance).

CONCLUSIONS AND OUTLOOK

In conclusion, the presented algorithm creates virtual individuals that are reasonable representatives of real healthy adults. Mean values and variabilities of the simulated plasma concentration time profiles in two virtual

simulations after intravenous administration very well matched the experimentally observed plasma concentration time profiles of ciprofloxacin and paclitaxel, demonstrating that the population model is able to simulate the variability due to distribution and elimination of these two drugs.

Potential applications of this population PBPK approach in the drug research and development environment include an estimation of the expected range of human pharmacokinetic profiles prior to Phase I studies, provided that reasonable estimates of the human clearance are available (e.g., via allometric scaling of laboratory animal clearances or from *in vitro* measurements such as intrinsic microsomal or hepatocyte clearance). After Phase I studies, the described model has the potential to aid in interpreting and understanding unexpected clinical outcomes, and providing initial pharmacokinetic predictions in certain sub-populations such as obese people, children, elderly, or patients suffering from pathological diseases.

REFERENCES

1. E. I. Ette and P. J. Williams. Population pharmacokinetics I: background, concepts, and models. *Ann. Pharmacother*. **38**(10):1702–1706 (2004).
2. S. Willmann, J. Lippert, M. Sevestre, J. Solodenko, F. Fois, and W. Schmitt. PK-Sim®: a physiologically based pharmacokinetic 'whole-body' model. *Biosilico*. **1**(4):121–124 (2003).
3. P. Poulin and F. P. Theil. A priori prediction of tissue: plasma partition coefficients of drugs to facilitate the use of physiologically-based pharmacokinetic models in drug discovery. *J. Pharm. Sci*. **89**(1):16–35 (2000).
4. S. Bjorkman. Prediction of drug disposition in infants and children by means of physiologically based pharmacokinetic (PBPK) modelling: theophylline and midazolam as model drugs. *Br. J. Clin. Pharmacol*. **59**(6):691–704 (2005).
5. G. Ginsberg, D. Hattis, and B. Sonawane. Incorporating pharmacokinetic differences between children and adults in assessing children's risks to environmental toxicants. *Toxicol. Appl. Pharmacol*. **198**(2):164–183 (2004).
6. F. P. Theil, T. W. Guentert, S. Haddad, and P. Poulin. Utility of physiologically based pharmacokinetic models to drug development and rational drug discovery candidate selection. *Toxicol. Lett*. **138**(1–2):29–49 (2003).
7. S. Willmann, J. Lippert, and W. Schmitt. From physicochemistry to absorption and distribution: predictive mechanistic modelling and computational tools. *Expert Opin. Drug. Meta. Toxicol*. **1**(1):159–168 (2005).
8. W. Schmitt and S. Willmann. Physiology-based pharmacokinetic modeling: ready to be used. *Drug Discovery Today: Technologies*. **2**(1):125–132 (2005).
9. P. S. Price, R. B. Conolly, C. F. Chaisson, E. A. Gross, J. S. Young, E. T. Mathis, and D. R. Tedder. Modeling interindividual variation in physiological factors used in PBPK models of humans. *Crit. Rev. Toxicol*. **33**(5):469–503 (2003).
10. A. N. Edginton, S. Willmann, and W. Schmitt. Development and validation of a generic physiology-based pharmacokinetic (PBPK) model for children. *Clin. Pharmacokinet*. **45**:1013–1034 (2006).
11. M. W. Haerter, J. Keldenich, and W. Schmitt. Estimation of physicochemical and ADME parameters. In: K. C. Nicolaou, R. Hanki, and W. Hartwig (eds.) *Handbook of Combinatorial Chemistry: Drugs, Catalysts, Materials*, Vol. 2. Wiley-VCH Verlag GmbH, Weinheim, Germany. pp 743–760 (2002).

12. J. Keldenich, W. Schmitt, and S. Willmann. A physiological/mechanistical model for predicting organ/plasma partitioning and volume of distribution. LogP2004 – The 3rd Lipophilicity Symposium, Zurich, Switzerland. Feb 29 to Mar 4, (2004).
13. Third National Health and Nutrition Examination Survey (NHANES III). 1997. National Center for Health Statistics Hyattsville, MD 20782 USA. http://www.cdc.gov/nchs/nhanes.htm. (1997).
14. International Commission on Radiological Protection (ICRP). *Basic Anatomical and Physiological Data for Use in Radiological Protection: Reference Values*. ICRP Publication 89. Elsevier Science, Amsterdam, The Netherlands (2002).
15. L. Sachs. Angewandte Statistik, 11. Auflage. Springer Verlag GmbH, Heidelberg, Deutschland (2003).
16. G. L. de la Grandmaison, I. Clairand, and M. Durigon. Organ weight in 684 adult autopsies: new tables for a Caucasoid population. *Forensic. Sci. Int*. **119**(2):149–154 (2001).
17. D. DuBois and E. F. DuBois. A formula to estimate the approximate surface area if height and weight be known. *Arch. Int. Med*. **17**:863–871 (1916).
18. G. B. Haycock, G. J. Schwartz, D. H. Wisotsky. Geometric method for measuring body surface area: a height weight formula validated in infants, children and adults. *J. Pediatr*. **93**:1:62–66 (1978).
19. E. A. Gehan, S. L. George. Estimation of human body surface area from height and weight. *Cancer. Chemother. Rep*. **54**:225–35 (1970).
20. R. D. Mosteller. Simplified Calculation of Body Surface Area. *N. Engl. J. Med*. **317**(17):1098 (letter) (1987).
21. H. W. Hense, B. Gneiting, M. Muscholl, U. Broeckel, B. Kuch, A. Doering, G.A. Riegger, and H. Schunkert. The associations of body size and body composition with left ventricular mass: impacts for indexation in adults. *J. Am. Coll. Cardiol*. **32**(2):451–457 (1998).
22. M. S. Lauer, K. M. Anderson, M. G. Larson, and D. Levy. A new method for indexing left ventricular mass for differences in body size. *Am. J. Cardiol*. **74**(5):487–491 (1994).
23. P. R. Stanforth, A. S. Jackson, J. S. Green, J. Gagnon, T. Rankinen, J. P. Despres, C. Bouchard, A. S. Leon, D. C. Rao, J. S. Skinner, and J. H. Wilmore. Generalized abdominal visceral fat prediction models for black and white adults aged 17–65 y: the HERITAGE Family Study. *Int. J. Obes. Relat. Metab. Disord*. **28**(7):925–932 (2004).
24. P. Gimondo, P. Mirk, B. A. La, G. Messina, and C. Pizzi. Sonographic estimation of fetal liver weight: an additional biometric parameter for assessment of fetal growth. *J. Ultrasound. Med*. **14**(5):327–333 (1995).
25. L. L. Maroun and N. Graem. Autopsy standards of body parameters and fresh organ weights in nonmacerated and macerated human fetuses. *Pediatr. Dev. Pathol*. **8**(2):204–217 (2005).
26. K. E. Bergmann, R. L. Bergmann, K. R. Von, O. Bohm, R. Richter, J. W. Dudenhausen, and U. Wahn. Early determinants of childhood overweight and adiposity in a birth cohort study: role of breast-feeding. *Int. J. Obes. Relat. Metab. Disord*. **27**(2):162–172 (2003).
27. E. M. Urbina, S. S. Gidding, W. Bao, A. S. Pickoff, K. Berdusis, and G. S. Berenson. Effect of body size, ponderosity, and blood pressure on left ventricular growth in children and young adults in the Bogalusa Heart Study. *Circulation* **91**(9):2400–2406 (1995).
28. D. C. Frankenfield, W. A. Rowe, R. N. Cooney, J. S. Smith, and D. Becker. Limits of body mass index to detect obesity and predict body composition. *Nutrition* **17**(1):26–30 (2001).
29. J. P. Clarys, S. Provyn, and M. J. Marfell-Jones. Cadaver studies and their impact on the understanding of human adiposity. *Ergonomics* 48(11–14):1445–1461 (2005).
30. S. Willmann, W. Schmitt, J. Keldenich, J. Lippert, and J. B. Dressman. A physiological model for the estimation of the fraction dose absorbed in humans. *J. Med. Chem.* **47**(15):4022–4031 (2004).

31. J. G. Hardman, L. E. Limbird, and A. Gilman. *Goodman and Gilman's: The Pharmacological Basis of Therapeutics*, 10th ed. McGraw Hill, New York (2001).
32. A. Shah, J. Lettieri, A. Heller, L. Kaiser, S. Collins, and J. Birkett. Pharmacokinetics of IV ciprofloxacin in subjects with normal renal function and with various degrees of renal impairment. Internal Report No. R6098 (1993).
33. A. Shah, J. Lettieri, R. Blum, S. Millikin, D. Sica, and A. H. Heller. Pharmacokinetics of intravenous ciprofloxacin in normal and renally impaired subjects. *J. Antimicrob. Chemother*. **38**(1):103–116 (1996).
34. F. Sorgel, K. G. Naber, U. Jaehde, A. Reiter, R. Seelmann, and G. Sigl. Gastrointestinal secretion of ciprofloxacin. Evaluation of the charcoal model for investigations in healthy volunteers. *Am. J. Med*. **87**(5A):62S–65S (1989).
35. M. T. Granfors, J. T. Backman, M. Neuvonen, and P. J. Neuvonen. Ciprofloxacin greatly increases concentrations and hypotensive effect of tizanidine by inhibiting its cytochrome P450 1A2-mediated presystemic metabolism. *Clin. Pharmacol. Ther*. **76**(6):598–606 (2004).
36. J. L. Dorne, K. Walton, and A. G. Renwick. Uncertainty factors for chemical risk assessment: human variability in the pharmacokinetics of CYP1A2 probe substrates. *Food. Chem. Toxicol*. **39**(7):681–696 (2001).
37. J. L. Dorne, K. Walton, and A. G. Renwick. Human variability in the renal elimination of foreign compounds and renal excretion-related uncertainty factors for risk assessment. *Food. Chem. Toxicol*. **42**:275–298 (2004).
38. V. R. Panday, W. W. ten Bokkel Huinink, J. B. Vermorken, H. Rosing, F. J. Koopman, M. Swart, J. H. Schellens, and J. H. Beijnen. Pharmacokinetics of paclitaxel administered as a 3-hour or 96-hour infusion. *Pharmacol. Res*. **40**(1):67–74 (1999).
39. H. J. van den Bongard, E. M. Kemper, T. O. van, H. Rosing, R. A. Mathot, J. H. Schellens, and J. H. Beijnen. Development and validation of a method to determine the unbound paclitaxel fraction in human plasma. *Anal. Biochem*. **324**(1):11–15 (2004).
40. S. Callies, D. P. de Alwis, A. Harris, P. Vasey, J. H. Beijnen, J. H. Schellens, M. Burgess, and L. Aarons. A population pharmacokinetic model for paclitaxel in the presence of a novel P-gp modulator, Zosuquidar Trihydrochloride (LY335979). *Br. J Clin. Pharmacol*. **56**(1):46–56 (2003).
41. R. Vaclavikova, S. Horsky, P. Simek, and I. Gut. Paclitaxel metabolism in rat and human liver microsomes is inhibited by phenolic antioxidants. *Naunyn Schmiedebergs Arch Pharmacol*. **368**(3):200–209 (2003).
42. J. L. Dorne, K. Walton, and A. G. Renwick. Human variability in CYP3A4 metabolism and CYP3A4-related uncertainty factors for risk assessment. *Food. Chem. Toxicol*. **41**(2):201–224 (2003).
43. A. J. MacDonald, A. Rostami-Hodjegan, G. T. Tucker and D. A. Linkens. Analysis of solvent central nervous system toxicity and ethanol interactions using a human population physiologically based kinetic and dynamic model. *Regul. Toxicol. Pharmacol*. **35**(2 Pt 1):165–76 (2002).
44. F. Jonsson and G. Johanson. Physiologically based modeling of the inhalation kinetics of styrene in humans using a bayesian population approach. *Toxicol. Appl. Pharmacol*. **15**(1):35–49 (2002).
45. F. Jonsson, F. Y. Bois and G. Johanson. Assessing the reliability of PBPK models using data from methyl chloride-exposed, non-conjugating human subjects. *Arch. Toxicol*. **75**(4):189–99 (2001).
46. F. Jonsson and G. Johanson. Bayesian estimation of variability in adipose tissue blood flow in man by physiologically based pharmacokinetic modeling of inhalation exposure to toluene. *Toxicology*. **157**(3):177–93 (2001).
47. L. M. Sweeney, T. R. Tyler, C. R. Kirman, R. A. Corley, R. H. Reitz, D. J. Paustenbach, J. F. Holson, M. D. Whorton, K. M. Thompson and M. L. Gargas. Proposed occupational exposure limits for select ethylene glycol ethers using PBPK models and Monte Carlo simulations. *Toxicol. Sci*. **62**(1):124–39 (2001).

48. S. S. Isukapalli, A. Roy and P. G. Georgopoulos. Stochastic response surface methods (SRSMs) for uncertainty propagation: application to environmental and biological systems. *Risk Anal*. **18**(3):351–63 (1998).
49. R. S. Thomas, W. E. Lytle, T. J. Keefe, A. A. Constan and R. S. Yang. Incorporating Monte Carlo simulation into physiologically based pharmacokinetic models using advanced continuous simulation language (ACSL): a computational method. *Fundam. Appl. Toxicol*. **31**(1):19–28 (1996).
50. H. J. Clewell 3rd and M. E. Andersen. Use of physiologically based pharmacokinetic modeling to investigate individual versus population risk. *Toxicology* **111**(1–3):315–29 (1996).
51. B. D. Beck, R. L. Mattuck, T. S. Bowers, J. T. Cohen and E. O'Flaherty. The development of a stochastic physiologically-based pharmacokinetic model for lead. *Sci. Total Environ*. **274**(1–3):15–9 (2001).
52. I. Gueorguieva, L. Aarons and M. Rowland. Diazepam pharmacokinetics from preclinical to phase I using a Bayesian population physiologically based pharmacokinetic model with informative prior distributions in Winbugs. *J. Pharmacokin. Pharmacodyn*. **33**(5):571–594 (2006).
53. G. Cheymol. Effects of obesity on pharmacokinetics. *Clin Pharmacokinet*. **39**(3):215–231 (2000).
54. S. F. La, R. Patti, E. Sciarrino, F. Valenza, G. S. Costanzo, L. Tese and R. Lagalla. Ultrasound, spleen and portal hypertension. *Radiol. Med (Torino)*. **107**(4):332–343 (2004).
55. N. Abramson and B. Melton. Leukocytosis: basics of clinical assessment. *Am. Fam. Physician* **62**(9):2053–2060 (2000).
56. D. L. Crandall, G. J. Hausman, and J. G. Kral. A review of the microcirculation of adipose tissue: anatomic, metabolic, and angiogenic perspectives. *Microcirculation* **4**(2):211–232 (1997).
57. P. Engfeldt and B. Linde. Subcutaneous adipose tissue blood flow in the abdominal and femoral regions in obese women: effect of fasting. *Int. J. Obes. Relat. Metab. Disord*. **16**(11):875–879 (1992).
58. G. Lesser and S. Deutsch. Measurement of adipose tissue blood flow and perfusion in man by uptake of ^{85}Kr. *J. Appl. Physiol*. **23**:621–623 (1967).
59. J. Alcorn and P. J. McNamara. Ontogeny of hepatic and renal systemic clearance pathways in infants: part I. *Clin. Pharmacokinet*. **41**(12):959–998 (2002).
60. B. J. Cusack. Pharmacokinetics in older persons. *Am. J. Geriatr. Pharmacother*. **2**(4):274–302 (2004).
61. J. A. Johnson. Predictability of the effects of race or ethnicity on pharmacokinetics of drugs. *Int. J. Clin. Pharmacol. Ther*. **38**(2):53–60 (2000).